https://doi.org/10.1016/j.apacoust.2018.11.032

Optimal design and experimental validation of sound absorbing multilayer microperforated panel with constraint conditions

Xiaocui Yang[a], Panfeng Bai[a], Xinmin Shen[a, b, *], Sandy To[b], Liang Chen[a, c, *], Xiaonan Zhang[a], Qin Yin[a]

[a]Department of Mechanical Engineering, College of Field Engineering, Army Engineering University, Nanjing, Jiangsu 210007, China;

[b]State Key Laboratory in Ultra-precision Machining Technology, Department of Industrial and Systems Engineering, The Hong Kong Polytechnic University, Hung Hom, Kowloon, Hong Kong SAR, China;

[c]Automobile NCO Academy, Army Military Transportation University, Bengbu, Anhui 233011, China.

Corresponding author: shenxmjfjlgdx2014@163.com; chenbb0708@163.com

Abstract. Sound absorption performance of the multilayer microperforated panel can be improved through optimal design of structural parameters. Theoretical model of sound absorbing coefficient of the multilayer microperforated panel with different layers was constructed according to Maa's theory. Structural parameters of the multilayer microperforated panel with layer number from 1 to 8 were optimized through the cuckoo search algorithm with constraint conditions. Preliminary verifications of the achieved optimal parameters were conducted by the analog simulation according to the finite element method. The obtained optimal design of multilayer microperforated panel with no more than 4 layers was finally validated by testing experiments based on the standing wave method, and the optimal average sound absorbing coefficients in the frequency range of 100-6000 Hz were 57.21%, 66.29%, 68.33%, and 69.36%, respectively. Through theoretical modeling, parameter optimization, analog simulation, and experimental validation, an effective method for development of the desired sound absorber was proposed, which will be propitious to promote the applications of the multilayer microperforated panel products in the field of noise reduction.

Keywords: multilayer microperforated panel; optimal design; sound absorbing coefficient; Cuckoo search algorithm; analog simulation; experimental validation.

1. Introduction

Microperforated panel is considered as a promising absorber for the noise reduction, because it has the advantages of an excellent sound absorption performance, high strength, fine washability, elegant appearance, outstanding machinability, and low manufacturing cost [1-3]. Under the same thickness condition, microperforated panel has a larger sound absorbing frequency band than the porous metals [4, 5]. Meanwhile, the microperforated panel made of metal presents a better flame resistance and dimensional stability relative to the polyester fiber [6, 7]. Moreover, low-frequency sound absorption performance of the microperforated panel was better than that of the porous material with the same limited thickness [8]. Optimization of microperforated panel was easier relative to that of polyester fiber or that of porous material, because it was mainly determined by the structural parameters and had little relationship with properties of the material [9]. Along with improvement of the precision machining technique and development of the lightweight metal material, the microperforated panel absorber has obtained more and more applications in the cinema, recording studio, conference room, opera house, factory workshop, family bedroom, and so on [10-12], which make it a research focus in the fields of architectural acoustics, material engineering, and design science [13, 14].

Since the microperforated panel was firstly developed by Maa [15, 16], many researches had been conducted to improve its sound absorption performance. Ning et al. [17] had studied acoustic properties of the microperforated panel absorber with arbitrary cross-sectional perforations, and the result indicated that the absorber with the triangle cross section achieved the largest sound absorbing coefficient and the highest sound absorption bandwidth. Qian et al. [18] had developed a strategy for

extending the effective application of microperforated panel absorbers to high sound intensity. Zhao et al. [19] had enhanced low-frequency sound absorption of the microperforated panel absorbers by combining parallel mechanical impedance. Liu et al. [20] had fabricated the porous polycarbonate material by additive manufacturing, and sound absorption properties of the sample were investigated. These studies improved sound absorption performance of the single layer microperforated panel.

However, the single layer microperforated panel has the ineluctable disadvantage of a limited sound absorption bandwidth according to the Maa's theory [15, 16]. The multilayer microperforated panel had been developed to enlarge the sound absorption bandwidth. Bravo et al. [21] had investigated the sound absorption properties of multilayer structures made up of the thin microperforated panels and developed a theoretical model formulation. Ruiz et al. [22] had conducted parameter optimization of the multiple-layer microperforated panels by simulated annealing. Zhao et al. [23, 24] had compared the calculation methods for absorptivity of multilayer microperforated panel absorber and optimized parameters of a microperforated panel with 3 layers by the genetic algorithm. Wang et al. [25] had investigated sound absorption property of parallel arrangement of the multiple microperforated panel absorbers in a periodic pattern and developed a 3D finite element model to simulate the acoustic behaviors. Results obtained in these studies indicated that the multilayer microperforated panel could achieve a larger sound absorption bandwidth, which promoted its applications in many fields.

Meanwhile, the present optimization works on sound absorption performance of the porous materials supplied references for the optimization of the multilayer microperforated panel. Optimization of the acoustic property of the graded semi-open cellular metal was conducted by Meng et al. [26] through adopting the genetic algorithm method. Structure of the porous metal fibrous material was optimized by Ao et al. [27] through changing the preparation processing and the structure parameters. A fractal

micro-structural acoustic model for sound absorption of sintered fibrous metals was established by Chen et al. [28] through using the fractal geometric theory. A mathematical model was constructed by Liu et al. [29] to obtain the optimized micro-structure design of porous fibrous material, with fiber radius and gap as design parameters and average absorption performance under set frequency band as target. The effects of gradient pore structure on the sound absorption performance of metal fiber porous materials were investigated by Zhu et al. [30], and the results indicated that the direction and quantity of the pore gradient interface exhibited remarkable effects.

In general, the present researches for the optimal sound absorption performance through optimizing parameters of the multilayer microperforated panel and those by optimizing parameters of the porous materials mainly focused on the sound absorption mechanism, and many theoretical models had been developed on foundation of the Maa's theory [15, 16] and the classical Johnson-Champoux-Allard model [26-30], respectively. Although there were some parameter optimizations for the multilayer microperforated panel and for the porous materials by the intelligent algorithm in some studies, they were only theoretical optimizations, which had not taken the practical application into consideration. In most cases, the available space for installation of the sound absorber is finite, which indicates that the dimension of the sound absorber should be limited. Therefore, optimal design and experimental validation of the sound absorbing multilayer microperforated panel with the constraint conditions was conducted in this research. Theoretical model of sound absorbing coefficient of the multilayer microperforated panel was constructed firstly based on the Maa's theory [15, 16]. Secondly, optimization of parameters of the multilayer microperforated panel was realized by the Cuckoo search algorithm [31, 32]. Thirdly, preliminary verifications of the achieved optimal parameters were conducted by the analog simulation according to the finite element method [33, 34]. Finally, the

obtained optimal design of multilayer microperforated panel was validated by the testing experiments based on the standing wave method [35, 36]. Through the theoretical modeling, analog simulation, and the experimental validation, optimal design of the multilayer microperforated panel was realized, which would improve its sound absorption performance and promote its application.

2. Theoretical modeling

Schematic diagram of structures of the multilayer microperforated panel is shown in Fig. 1. Total layer of the multilayer microperforated panel is n. Distribution of the holes in this study is square array. For the i layer, diameter of the hole, thickness of the panel, distance of the neighboring hole, and length of the cavity are symbolized by d_i, t_i, b_i, and D_i, respectively.

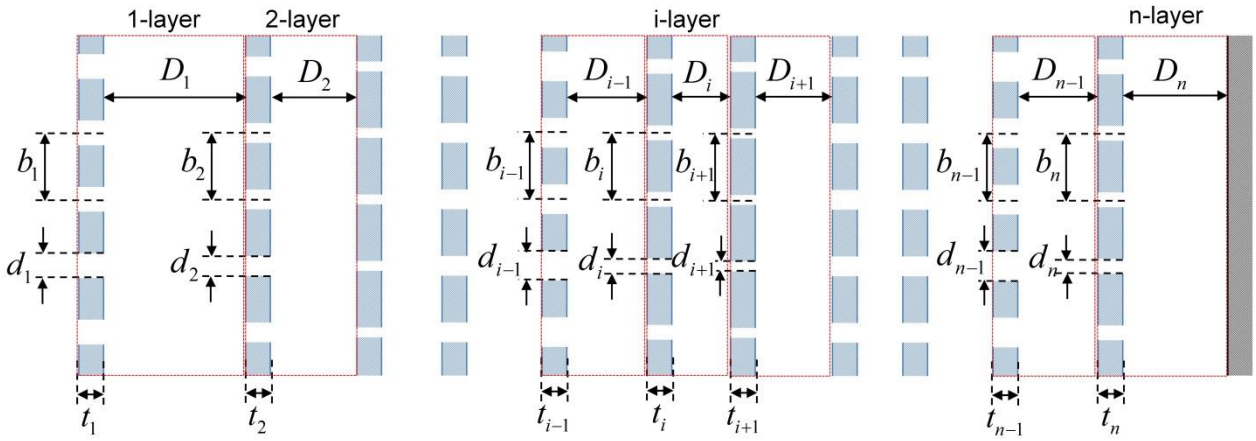

Fig. 1. Schematic diagram of structures of the multilayer microperforated panel

Based on the Maa's theory [1, 15, 16], sound absorbing coefficient of the multilayer microperforated panel can be derived according to the transfer matrix method [23, 37, 38]. With regard to the i layer microperforated panel, its acoustic impedance Zs_i can be represented by Eq. 1, and the real part R_i and imaginary part X_i can be calculated by Eq. 2 and Eq. 3, respectively [15, 39].

$$Zs_i = R_i + jX_i \tag{1}$$

$$R_i = \frac{32(\mu+\upsilon)\rho}{\varepsilon_i}\frac{t_i}{d_i^2}kr_i \tag{2}$$

$$X_i = \frac{t_i \omega \rho}{\varepsilon_i} km_i \tag{3}$$

Here μ is viscosity coefficient of the air, $1.506 \cdot 10^{-5}$ m^2/s; υ is temperature conduction coefficient of the metal panel, $2.0 \cdot 10^{-5}$ m^2/s; ρ is density of the air, 1.225 kg/m^3; ε_i is the perforating rate, which can be calculated by Eq. 4; kr_i is the acoustic resistance constant, which can be obtained by Eq. 5; ω is the angular frequency, which can be achieved by Eq. 6; km_i is the acoustic mass constant, which can be derived by Eq. 7 [15, 39]. In Eq. 5 and Eq. 7, k_i is the perforated panel constant, which can be calculated by Eq. 8. In Eq. 6, f is the sound frequency.

$$\varepsilon_i = \frac{\pi}{4} \left(\frac{d_i}{b_i} \right)^2 \tag{4}$$

$$kr_i = \sqrt{1 + \frac{k_i^2}{32}} + \frac{\sqrt{2}}{8} k_i \frac{d_i}{t_i} \tag{5}$$

$$\omega = 2\pi f \tag{6}$$

$$km_i = 1 + \frac{1}{\sqrt{9 + \frac{k_i^2}{2}}} + 0.85 \frac{d_i}{t_i} \tag{7}$$

$$k_i = \sqrt{\frac{\omega}{\mu + \upsilon}} \frac{d_i}{2} \tag{8}$$

Transfer matrix P_i of the i layer microperforated panel and that S_i of the corresponding i layer cavity can be represented by Eq. 9 and Eq. 10, respectively [15, 39]. In Eq. 10, j is imaginary unit, and c is sound speed in the air, 340 m/s. Thus, with regard to the multilayer microperforated panel, the total transfer matrix T is the sequential multiplying of transfer matrix P_i of each panel and that S_i of the cavity, as shown in the Eq. 11. Through this transfer matrix method, sound absorbing coefficient α of the multilayer microperforated panel can be obtained, as shown in Eq. 12 [15, 39].

$$[P_i] = \begin{bmatrix} 1 & Zs_i \\ 0 & 1 \end{bmatrix} \tag{9}$$

$$[S_i]=\begin{bmatrix} \cos\left(\frac{\omega}{c}D_i\right) & j\rho c\sin\left(\frac{\omega}{c}D_i\right) \\ \frac{j}{\rho c}\sin\left(\frac{\omega}{c}D_i\right) & \cos\left(\frac{\omega}{c}D_i\right) \end{bmatrix} \tag{10}$$

$$[T]=\prod_{i=1}^{n}[P_i][S_i]=[P_1][S_1]...[P_i][S_i]...[P_n][S_n]=\begin{bmatrix} T_{11} & T_{12} \\ T_{21} & T_{22} \end{bmatrix} \tag{11}$$

$$\alpha=\frac{4\,\mathrm{Re}\left(\frac{T_{11}}{\rho cT_{21}}\right)}{\left[1+\mathrm{Re}\left(\frac{T_{11}}{\rho cT_{21}}\right)\right]^2+\left[\mathrm{Im}\left(\frac{T_{11}}{\rho cT_{21}}\right)\right]^2} \tag{12}$$

3. Parameter optimization

From the theoretical modeling process, it can be observed that sound absorption performance of the multilayer microperforated panel is determined by its structural parameters, which include diameter of the hole, thickness of the panel, distance of the neighboring hole, and length of the cavity of each layer. With regard to the multilayer microperforated panel with n layers, there are $4n$ parameters. Therefore, optimization of the dimensional parameters is a significant procedure to improve sound absorbing coefficient of the multilayer microperforated panel. The available ranges of diameter of the hole d_i, thickness of the panel t_i, and distance of the neighboring hole b_i are shown in Eq. 13, which are the normal value ranges for the common microperforated panel [1, 15, 39].

$$\begin{cases} 1\square 10^{-4}m \le d_i \le 1\square 10^{-3}m \\ 1\square 10^{-4}m \le t_i \le 2\square 10^{-3}m \\ 1\square 10^{-3}m \le b_i \le 1\square 10^{-2}m \end{cases} \tag{13}$$

Total size of the multilayer microperforated panel L is summation of the thicknesses of all panels and the lengths of all cavities, as shown in Eq. 14. Thickness of each panel t_i is smaller than length of the cavity D_i, so L is mainly determined by the summation of lengths of all cavities $\sum_{i=1}^{n}(D_i)$.

$$L=\sum_{i=1}^{n}(t_i+D_i)\approx\sum_{i=1}^{n}(D_i) \tag{14}$$

In most cases, total size of the multilayer microperforated panel L is limited, which is decided by available space of the target required noise reduction. Taking this limit into consideration, the added constraint conditions are shown in Eq. 15, and L_0 represents the limit.

$$\begin{cases} \sum_{i=1}^{n}(D_i) \le L_0 \\ 0 \le D_i \le L_0 \end{cases} \tag{15}$$

Aim of the parameter optimization is to achieve an optimal average sound absorbing coefficient in a certain frequency range $[f_{\min}, f_{\max}]$, as shown in Eq. 16.

$$\text{maximize}: average(\alpha(f)) \quad f \in [f_{\min}, f_{\max}] \tag{16}$$

Cuckoo search is a novel metaheuristic search algorithm, which is founded according to the obligate brood parasitic behavior of some cuckoo species in combination with the Levy flight behavior of some birds and fruit flies [31, 32, 40]. The cuckoo search algorithm has been shown to be effective in solving continuous optimization problems [41], which is applied in this study to optimize parameters of the multilayer microperforated panel. Pseudo codes of the standard Cuckoo search algorithm are shown in Table. 1 [31, 32, 40-42]. The Cuckoo search is summarized around the following ideal rules: (1) Each cuckoo lays one egg at a time and selects a nest randomly; (2) The best nest with the highest quality egg can pass onto the new generations; (3) The number of host nests is fixed, and the egg laid by a cuckoo can be discovered by the host bird with a probability $p_a \in [0,1]$. For a cuckoo i, a new solution $x_i^{(t+1)}$ is generated according to the Levy flight, as shown in Eq. 17.

$$x_i^{(t+1)} = x_i^{(t)} + \beta \oplus Levy(s, \lambda) \tag{17}$$

Here $\beta(\beta > 0)$ is the step size, and $\beta = O(1)$ can be used in many cases. The step length follows the Levy distribution, as shown in Eq. 18, which has an infinite variance with an infinite mean. Here s is step size drawn from a Levy distribution [31, 32, 40-42].

$$Levy(s,\lambda) \sim s^{-\lambda}, (\lambda \in (1,3]) \tag{18}$$

Table. 1 Pseudo codes of the standard Cuckoo search algorithm [31, 32, 40-42]

Cuckoo search algorithm
1: Objective function $f(x), x=(x_1,x_2,...,x_d)^T$;
2: Generate initial population of n host nests $x_i (i=1,2,...,n)$;
3: **while** ($t \le MaxGeneration$) or (stop criterion) **do**
4: Get a cuckoo (say, i) randomly and generate a new solution by Levy flights;
5: Evaluate its quality/fitness F_i;
6: Choose a nest among n (say, j) randomly;
7: **if** ($F_i \ge F_j$) **then**
8: replace j by the new solution;
9: **end if**
10: A fraction (P_a) of worse nests are abandoned and new ones are built at new locations;
11: Keep the best solutions (or nests with quality solutions);
12: Rand the solutions and find the current best;
13: **end while**
14: Postprocess results and visualization;

Taking a practical requirement for example, we had conducted optimization of the parameters by the Cuckoo search algorithm. The limit L_0 was 30 mm. The studied frequency range was 100-6000 Hz. The multilayer microperforated panels with layer number from 1 to 8 were investigated. Summarized results of the optimal design obtained by the Cuckoo search algorithm were shown in Table. 2.

Table. 2 Summarized results of the optimal design based on the Cuckoo search algorithm

Multilayer	Layer series	Diameter of the hole (mm)	Thickness of the panel (mm)	Distance of the hole (mm)	Length of the cavity (mm)	Optimal average sound absorbing coefficient (%)
1	1	0.149375	0.1	1	16.95656	69.79215336
2	1	0.23231	0.171794	1.000006	11.84933	84.30035381
	2	0.13534	0.1	1	18.15067	
3	1	0.847898	0.442586	2.441541	9.418376	85.52387103
	2	0.658632	1.359062	2.250937	6.053829	
	3	0.149	0.241174	1.051383	14.51047	
4	1	0.868148	0.505478	2.356235	9.948546	85.7409884
	2	0.726755	0.733495	2.952788	6.708019	
	3	0.758657	0.531005	4.468265	3.828585	
	4	0.159082	0.465277	1.182893	9.081581	
5	1	0.512036	1.395008	1.064705	10.99994	85.77246781
	2	0.910099	0.371717	4.110391	6.867025	
	3	0.765401	0.458938	4.717307	4.499401	
	4	0.459925	0.313601	4.50495	3.562259	
	5	0.231651	0.305109	3.295978	4.065623	
6	1	0.877683	1.336498	1.819496	8.475891	85.87223922
	2	0.809354	0.416281	1.008567	1.491759	
	3	0.422294	0.60942	1.885886	7.472921	
	4	0.603259	0.802133	3.396963	4.386888	
	5	0.469026	0.155058	5.410587	3.226398	
	6	0.219217	0.108154	4.45992	4.943848	
7	1	0.995307	0.120466	3.31102	9.513225	85.90581063
	2	0.624564	1.055358	2.357315	6.119821	
	3	0.84265	0.148826	4.412042	2.494081	
	4	0.943232	0.150462	5.432496	2.814387	
	5	0.405801	1.089907	1.64159	1.826852	
	6	0.718347	1.163026	4.260467	2.340624	
	7	0.154584	0.166304	2.268056	4.741549	
8	1	0.968626	0.197765	2.972917	9.233162	85.9778079
	2	0.914732	1.059007	2.687111	1.331626	
	3	0.825938	0.62169	1.440212	2.534271	
	4	0.895434	0.387228	3.050642	3.671668	
	5	0.680018	0.2835	3.555225	1.918827	
	6	0.780083	0.606854	3.981708	3.366674	
	7	0.437208	0.345036	4.261323	3.105886	
	8	0.198225	0.148417	3.317497	4.814089	

It could be observed from Table 2 that average sound absorbing coefficient of 69.79% for the 1 layer was significantly improved to that of 84.3% for 2 layers. Further increase of the layer number gained few improvement of the average sound absorbing coefficient. Especially when the layer number was larger than 4, raise of the average sound absorbing coefficient was smaller than 0.1% with the further increase of layer number. It was interesting to note that in some conditions, summation of lengths of all cavities is smaller than 30 mm. Taking the microperforated panel with 1 layer for example, the optimal cavity was 16.96 mm. Increase of length of the cavity would obtain a higher sound absorbing coefficient in the low frequency band, but the sound absorbing coefficient was decreased in the high frequency band, because the absorbing peak was moved to the low frequency direction. That's why the average sound absorbing coefficient was not raised along with increase of length of the cavity.

In order to comprehensive compare the evolutions of sound absorbing coefficients of the multilayer microperforated panel with different layers, the obtained optimal parameters were introduced into the theoretical models, and the achieved corresponding sound absorbing coefficients were shown in Fig. 2. It could be observed that except the result for 1 layer, the multilayer microperforated panels with more than 2 layers obtained high sound absorbing coefficients in the frequency ranges of 1000-6000 Hz, which indicated that the sound absorbing efficiency was improved by adding the layer numbers. Meanwhile, it could be noted that sound absorption performances of the multilayer microperforated panels with more than 2 layers were very close, no matter in the high frequency band or in the low frequency band, which were consistent with the results in Table 2. It indicated that optimal design of the multilayer microperforated panel should select an appropriate layer number, because increase of the layer numbers meant raise of the costs in design, manufacture, assembly, transport, installation, application, maintenance, and so on.

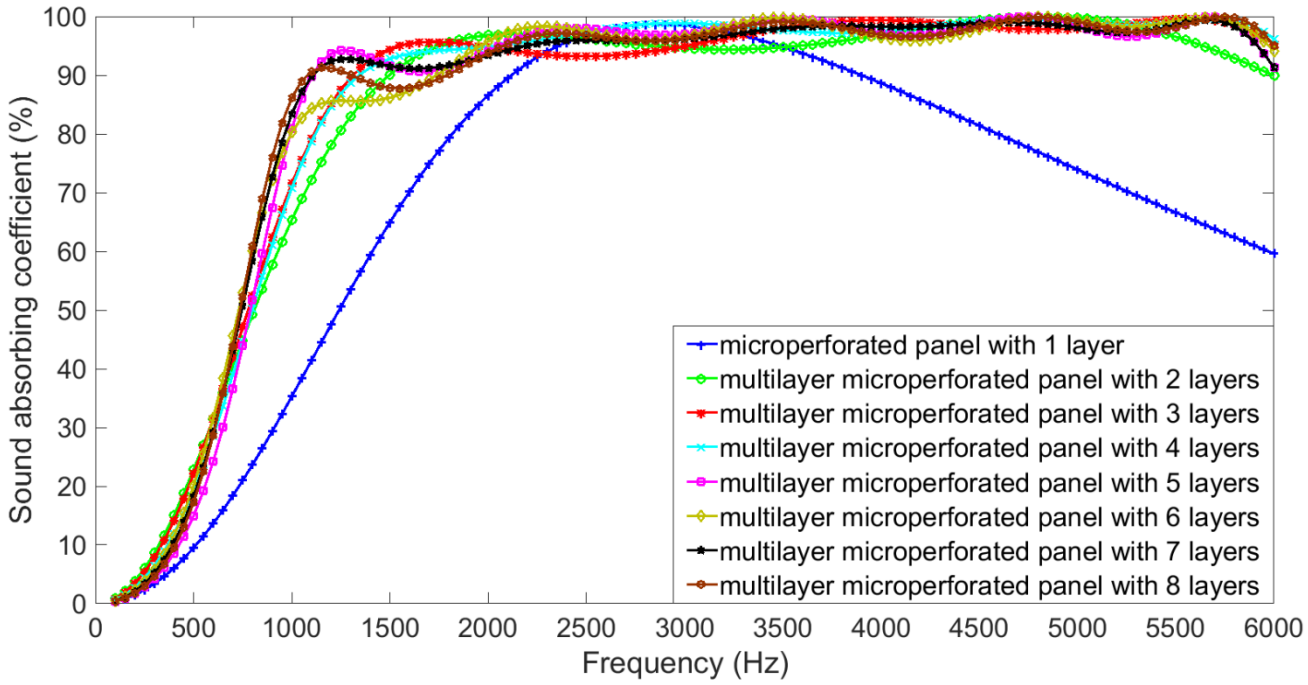

Fig. 2. Theoretical sound absorbing coefficients of the optimal design obtained by Cuckoo search

For the purpose of further comparing sound absorbing coefficients of the multilayer microperforated panels with more than 2 layers, detailed sound absorption performances in the frequency ranges of 1000-6000 Hz were shown in Fig. 3. It could be found that the starting sound absorbing coefficient in frequency 1000 Hz was gradually improved along with increase of the layer numbers. Meanwhile, the larger the layer number was, the smoother the change curve was. The maximum, minimum, and average values of sound absorbing coefficients of the multilayer microperforated panels with more than 2 layers in the frequency ranges of 1000-6000 Hz were summarized in Table 3. It could be found that the average sound absorbing coefficients were all larger than 90%. Especially when the layer number exceeded 5, minimum of the sound absorbing coefficient was larger than 80%, which exhibited an outstanding sound absorption performance. The major reason for this phenomenon was that each microperforated panel had its absorption band, and increase of the layer number indicated superposition of these absorption bands, which would obtain a better sound absorption performance in a wideband, especially in the high frequency range.

Table. 3 Comparisons of sound absorbing coefficients in the frequency ranges of 1000-6000 Hz

	2 layers	**3 layers**	**4 layers**	**5 layers**	**6 layers**	**7 layers**	**8 layers**
Maximum	99.96	99.69	99.57	99.99	99.87	99.39	99.97
Minimum	65.39	71.55	70.79	80.86	80.29	83.43	86.16
Average	94.46	95.74	96.33	96.52	95.84	96.07	96.07

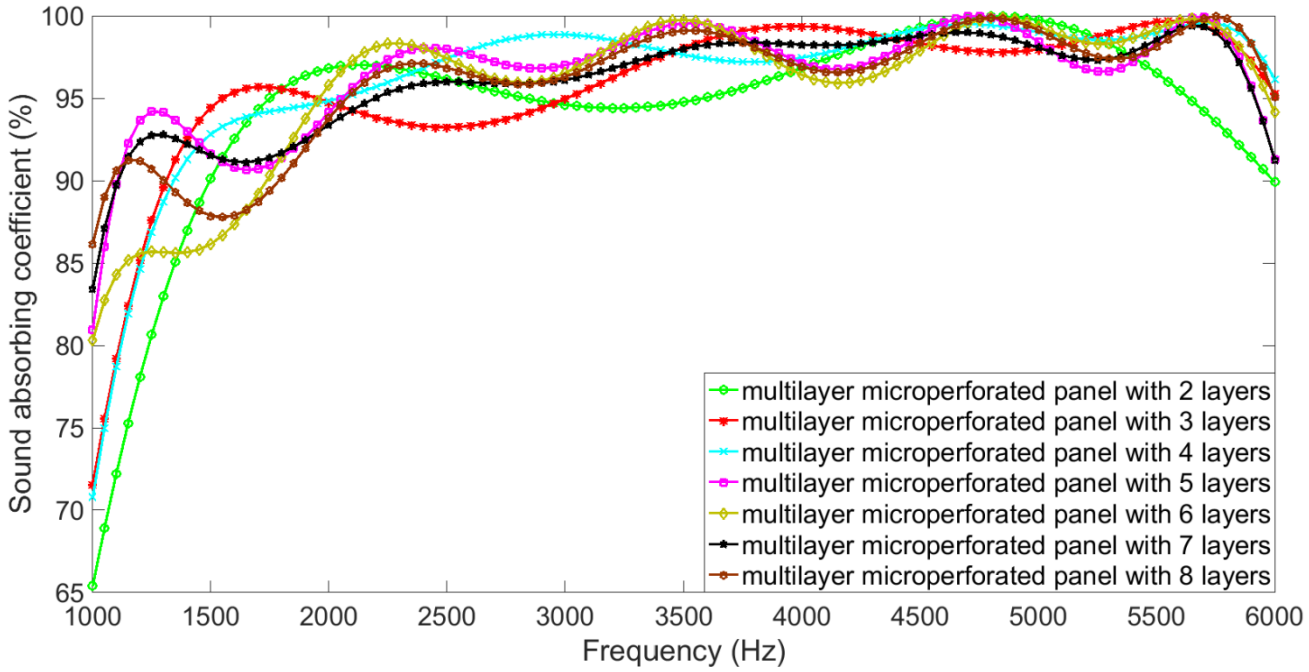

Fig. 3. Detailed sound absorption performances of the multilayer microperforated panels

4. Analog simulation

Preliminary verifications of the achieved optimal parameters for multilayer microperforated panels were obtained by analog simulation according to finite element method [33, 34], and the simulation model was constructed in the software LMS Virtual. Lab, as shown in Fig. 4. Plane wave was treated as the sound source, which was set in the acoustic source inlet. Real part and imaginary part of the constant values for the panel velocity boundary condition were 1 m/s and 0 m/s, respectively. The grid partition was obtained by 5 mm square elements. Each microperforated panel was represented by the corresponding acoustic transfer relation admittance between two surfaces. Two test points

were added on the tube to measure sound pressure of the incident wave and that of the reflected wave, which was used to calculate the sound absorbing coefficient for a certain frequency. The tube and the cavities in the model were realized by stretching of the gridding surface according to the structural parameters. For the multilayer microperforated panel with n layers, the n panels and n cavities were added in the simulation model respectively according to their parameters. In this way, sound absorption performances of the multilayer microperforated panels with n layers were simulated.

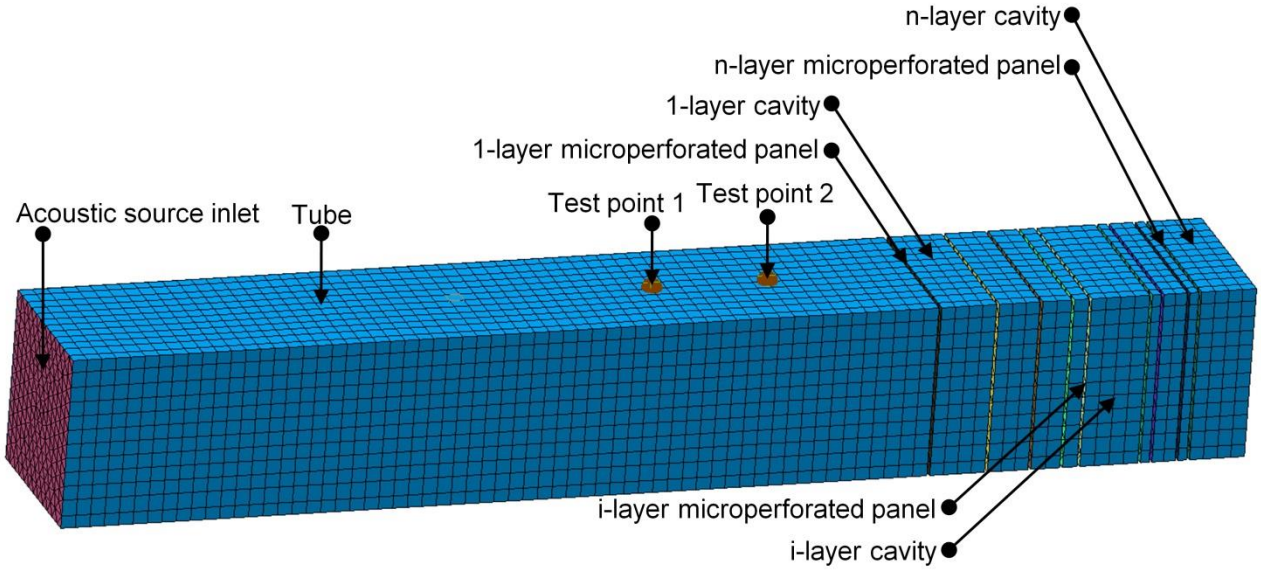

Fig. 4. Simulation model for sound absorption performance of the multilayer microperforated panel

Taking the manufacture cost and control accuracy into account, the optimal parameters obtained by Cuckoo search algorithm were handled by reducing the number of decimal digits, as shown in Table 4. Accuracies of diameter of the hole and thickness of the panel were kept 0.01 mm, and those of distance of the hole and length of the cavity were 0.1 mm. The obtained average sound absorbing coefficients of the multilayer microperforated panels with layers from 1 to 8 were 69.97%, 84.24%, 85.47%, 85.73%, 85.75%, 85.88%, 85.72%, and 86.04%, respectively. It could be found the achieved simulation results were almost consistent with the obtained theoretical results in Table. 2, and the differences between the simulation results and the theoretical results were reduced in ±0.2%. There

were two reasons for the generation of these differences. First was the computational error in the simulation process. Second was the parameter error by reducing the number of decimal digits.

Table. 4 Summarized results of the analog simulation according to the finite element method

Multilayer	Layer series	Diameter of the hole (mm)	Thickness of the panel (mm)	Distance of the hole (mm)	Length of the cavity (mm)	Optimal average sound absorbing coefficient (%)
1	1	0.15	0.10	1.0	17.0	69.97
2	1	0.23	0.17	1.0	11.8	84.24
	2	0.14	0.10	1.0	18.2	
3	1	0.85	0.44	2.4	9.4	85.47
	2	0.66	1.36	2.3	6.1	
	3	0.15	0.24	1.1	14.5	
4	1	0.87	0.51	2.4	9.9	85.73
	2	0.73	0.73	3.0	6.7	
	3	0.76	0.53	4.5	3.8	
	4	0.16	0.47	1.2	9.1	
5	1	0.51	1.40	1.1	10.9	85.75
	2	0.91	0.37	4.1	6.9	
	3	0.77	0.46	4.7	4.5	
	4	0.46	0.31	4.5	3.6	
	5	0.23	0.31	3.3	4.1	
6	1	0.88	1.34	1.8	8.5	85.88
	2	0.81	0.42	1.0	1.5	
	3	0.42	0.61	1.9	7.5	
	4	0.60	0.80	3.4	4.4	
	5	0.47	0.16	5.4	3.2	
	6	0.22	0.11	4.5	4.9	
7	1	1.00	0.12	3.3	9.5	85.72
	2	0.62	1.06	2.4	6.1	
	3	0.84	0.15	4.4	2.5	
	4	0.94	0.15	5.4	2.8	
	5	0.41	1.09	1.6	1.8	
	6	0.72	1.16	4.3	2.3	
	7	0.15	0.17	2.3	4.7	
8	1	0.97	0.20	3.0	9.2	86.04
	2	0.91	1.06	2.7	1.3	
	3	0.83	0.62	1.4	2.5	
	4	0.90	0.39	3.1	3.7	

5	0.68	0.28	3.6	1.9
6	0.78	0.61	4.0	3.4
7	0.44	0.35	4.3	3.1
8	0.20	0.15	3.3	4.8

Comparisons of the simulation results and theoretical results in frequency range 100-6000 Hz were shown in Fig. 5, and the detailed comparisons in high frequency band were shown in Fig. 6. It could be observed that both of them were consistent in each frequency point, and the differences were kept in ±2.5%, which preliminary verified the accuracy and effectiveness of the optimal design.

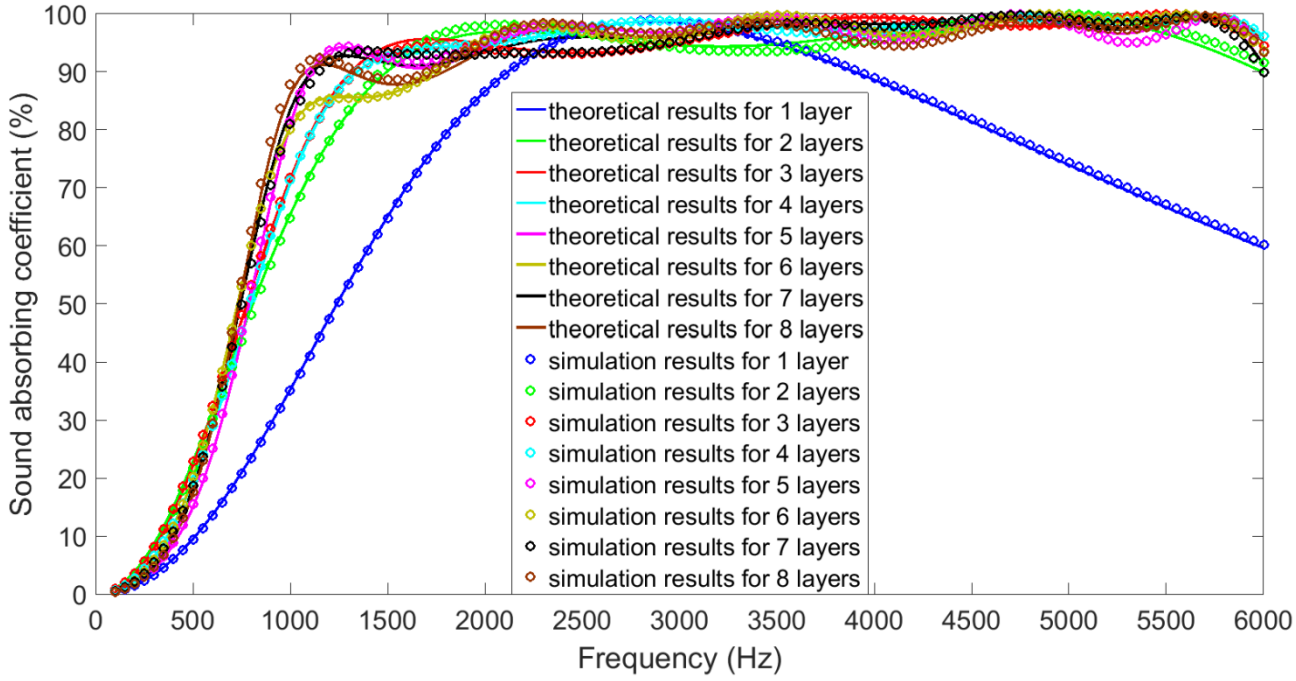

Fig. 5. Comparisons of the simulation results and theoretical results in frequency range 100-6000 Hz

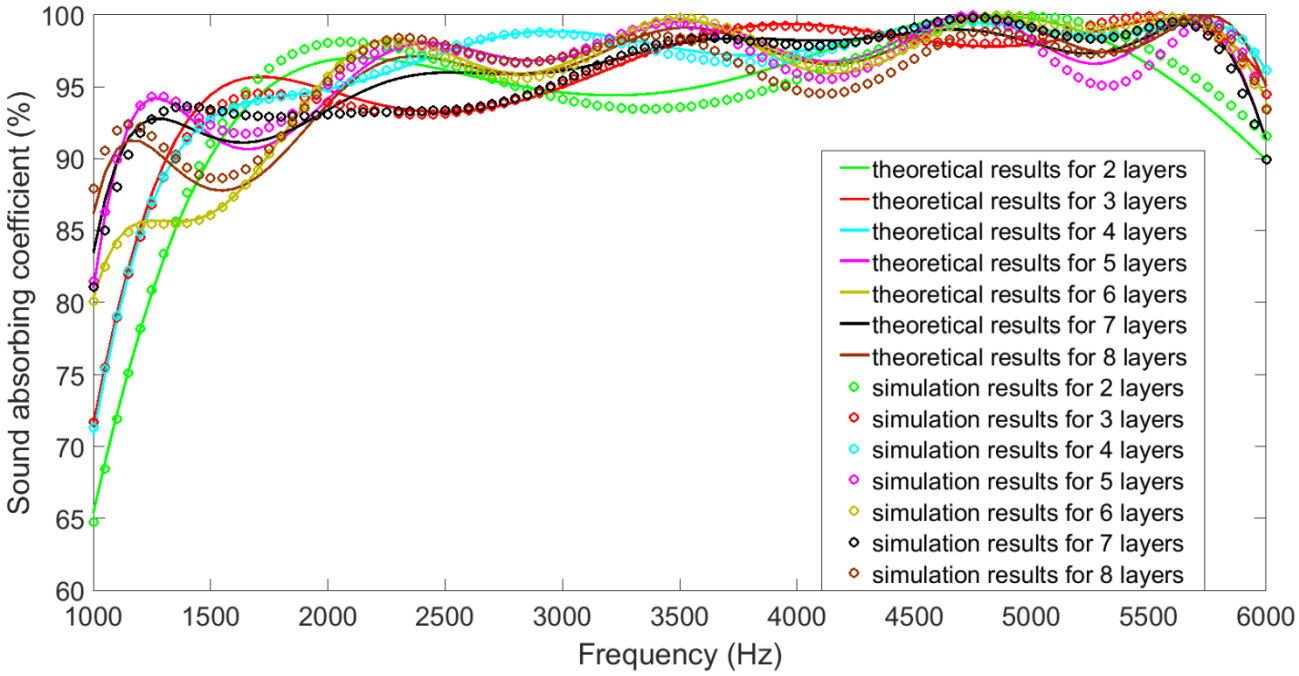

Fig. 6. Detailed comparisons of the simulation results and theoretical results in high frequency band

5. Experimental validation

In order to examine effectiveness of the optimal design, the further experimental validations of sound absorbing coefficients of the multilayer microperforated panel were conducted based on the standing wave method [35, 36]. In consideration of the structural complexity and the manufacturing cost, the obtained optimal multilayer microperforated panels with no more than 4 layers were tested. The detected microperforated panels were fabricated by laser beam drilling of the steel spring plate. In view of process capability and optional parameters of the machining equipment, the optimal diameter and distance of the holes in the microperforated panels obtained by Cuckoo search algorithm were further handled, as shown in Table 5. Meanwhile, thickness of each panel was also approximated by taking into account the common dimensions easy to purchase. Length of the cavity was controlled by the blocks with desired size fabricated by additive manufacturing. Illustrations of the investigated multilayer microperforated panels with no more than 4 layers were shown in Fig. 7.

Table. 5 Summarized results of the experimental validation based on the standing wave method

Multilayer	Layer series	Diameter of the hole (mm)	Thickness of the panel (mm)	Distance of the hole (mm)	Length of the cavity (mm)	Optimal average sound absorbing coefficient (%)
1	1	0.15	0.1	1.0	17.0	57.21
2	1	0.25	0.15	1.0	11.8	66.29
	2	0.15	0.1	1.0	18.2	
3	1	0.85	0.4	2.4	9.4	68.33
	2	0.65	1.5	2.3	6.1	
	3	0.15	0.25	1.1	14.5	
4	1	0.85	0.5	2.4	9.9	69.36
	2	0.75	0.7	3.0	6.7	
	3	0.75	0.5	4.5	3.8	
	4	0.15	0.5	1.2	9.1	

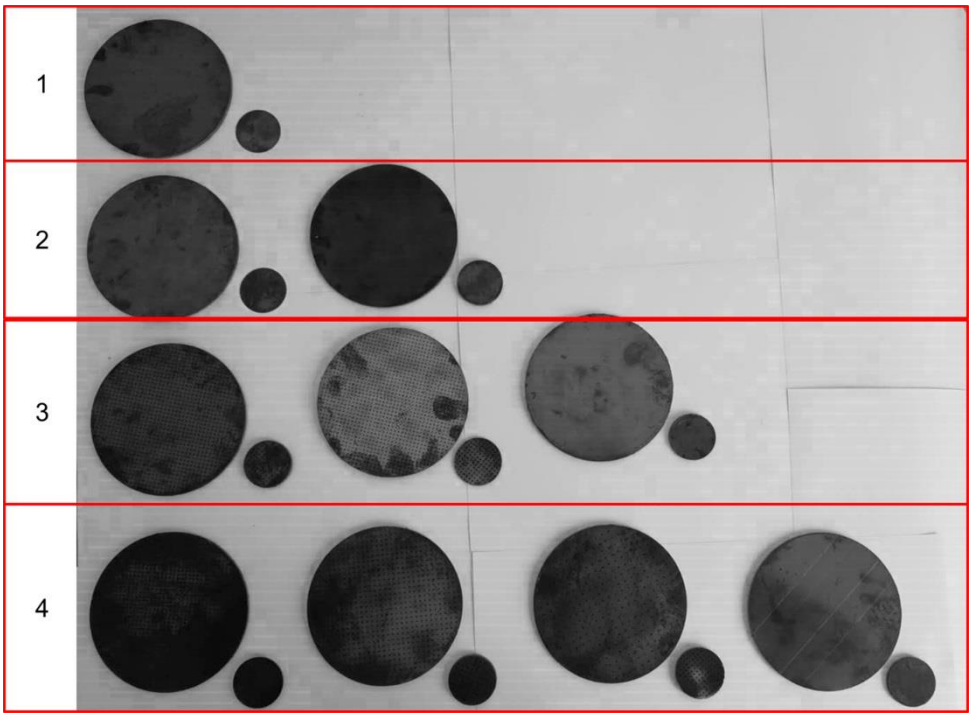

Fig. 7. Illustrations of the investigated multilayer microperforated panels

Afterwards, the investigated multilayer microperforated panels were tested by AWA6128A detector. Schematic diagram of the experimental system was shown in Fig. 8. The sound absorbing coefficient

α can be calculated by detections of peak sound level $L_{\max}$ and corresponding valley sound level $L_{\min}$ in a certain frequency [35], as shown in Eq. 19.

$$\alpha = \frac{4\square 10^{(L_{\max}-L_{\min})/20}}{\left(1+10^{(L_{\max}-L_{\min})/20}\right)^2} \tag{19}$$

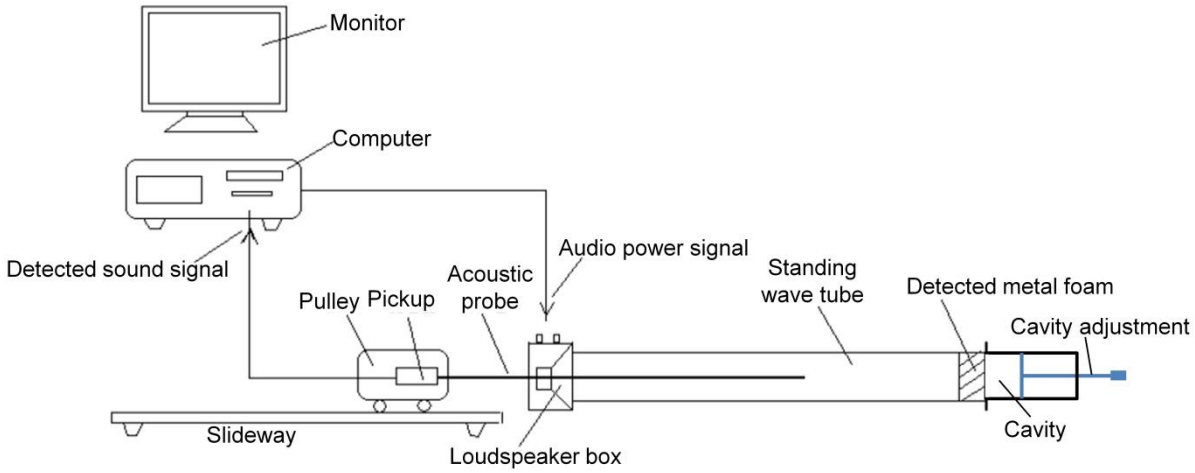

Fig. 8. Schematic diagram of the AWA6128A detector for measuring sound absorbing coefficient

The measurement was divided into two steps, because the measurement accuracy of sound absorbing coefficient is determined by diameter of the detected sample [35]. Therefore, for the measurement of sound absorbing coefficient in the frequency range of 100-1800 Hz, diameter of the detected sample is 96 mm. Accordingly, for the measurement of sound absorbing coefficient in the frequency range of 2000-6000 Hz, diameter of the detected sample is 30 mm. For each panel, dimensional parameters of the two samples were same, including diameter of the hole, thickness of the panel, an distance of the hole. That is why there were one big sample and one small sample for each panel in Fig. 7.

The obtained sound absorbing coefficients of the multilayer microperforated panels with no more than 4 layers were shown in Fig. 9. It could be found that evolution of sound absorbing coefficient was generally consistent with that of the theoretical data and that of the simulation data. The optimal average sound absorbing coefficients in the frequency range of 100-6000 Hz were 57.21%, 66.29%, 68.33%, and 69.36% corresponding to the multilayer microperforated panels with layer number of 1,

2, 3, and 4, respectively, which were also summarized in Table. 5. Comparing with the theoretical data in Table. 2 and simulation data in Table. 4, it could be found that the actual optimal average sound absorbing coefficients obtained in the experiments decreased, which could also be judged intuitively from the comparisons in Fig. 9. We supposed that there were three major reasons account for these differences. Firstly, there existed fabrication error in the preparation of the microperforated panels. Through comparing the theoretical optimal parameters in Table. 2 and the applied actual parameters in Table. 5, it could be observed that there were some tiny deviations, because process capability of the adopted machine was limited. Meanwhile, length of the cavity was difficult to be consistent with the theoretical values completely in the measurement process, which also affected the experimental results. Secondly, some factors were neglected or simplified in the theoretical modeling process and the analog simulation process, such as transmission efficiency of the heat conversed from the sound energy, influence of the air expansion caused by temperature promotion to the sound wave, and so on. These neglected or simplified factors also led to differences between the theoretical data and the actual data. Thirdly, test error in the measurement process was unavoidable, although each sample was measured for 10 times to minimize this error as much as possible.

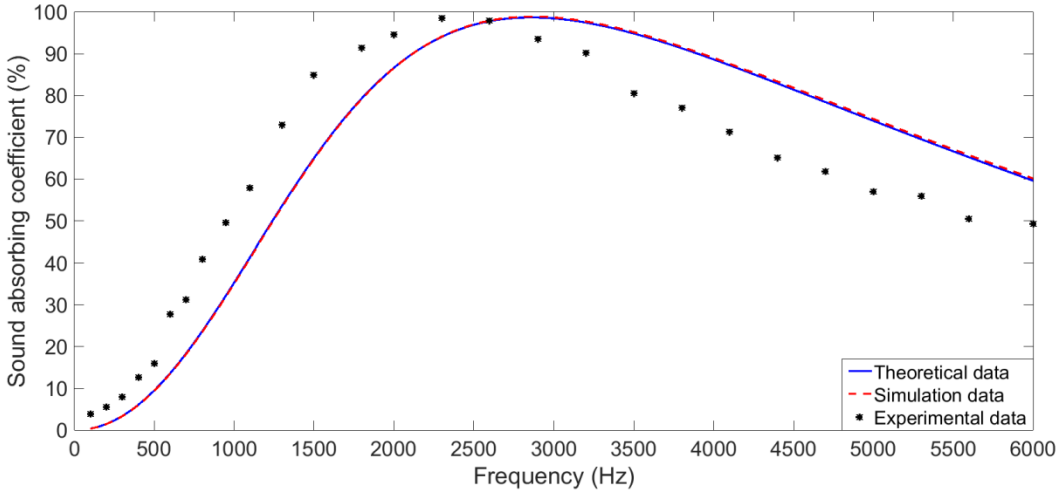

(a) Microperforated panel with 1 layer

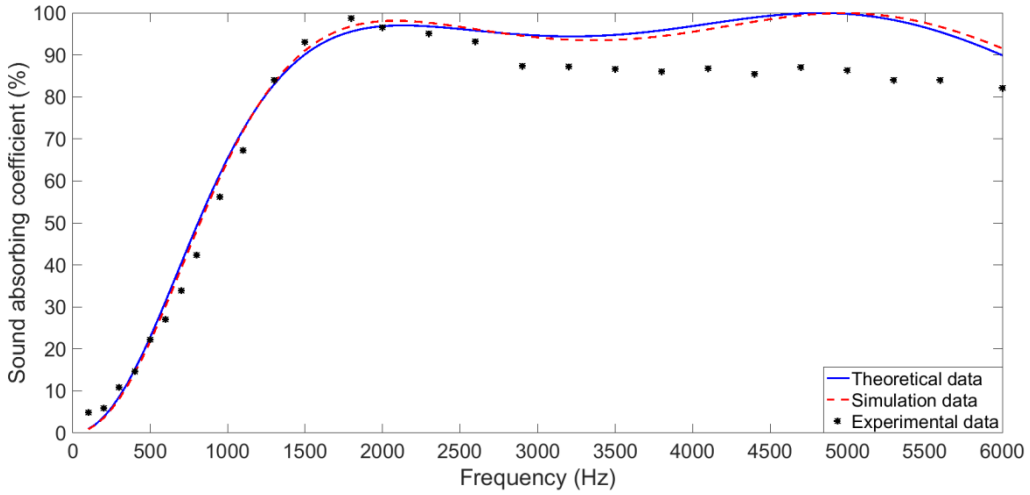

(b) Multilayer microperforated panel with 2 layers

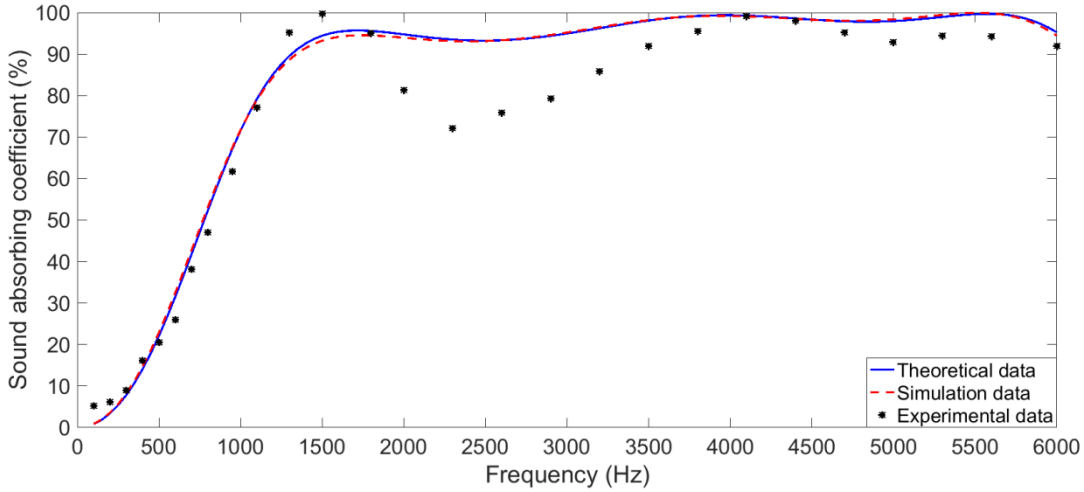

(c) Multilayer microperforated panel with 3 layers

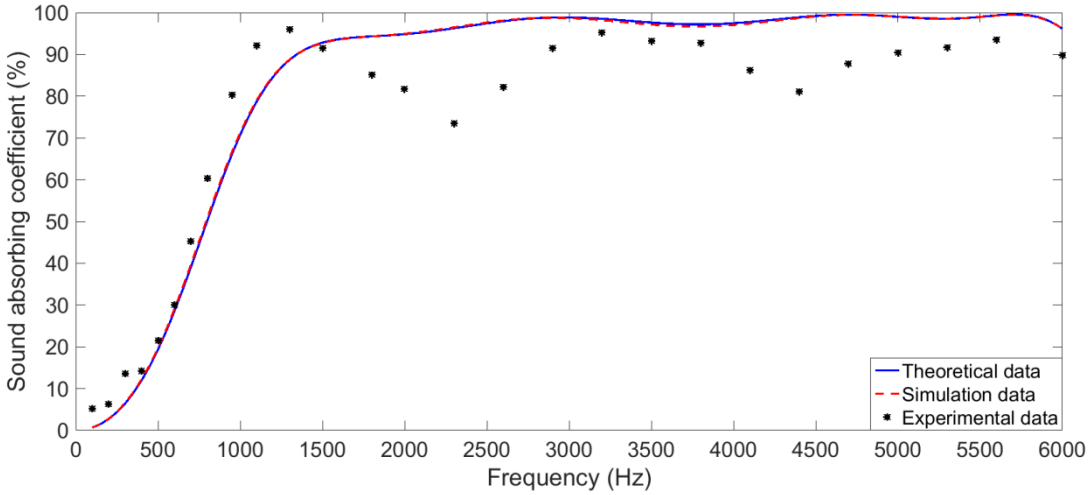

(d) Multilayer microperforated panel with 4 layers

Fig. 9. Comparisons of sound absorbing coefficients of the investigated multilayer microperforated panel among theoretical data, simulation data, and experimental data

It could be judged from Fig. 9 that deviations between the theoretical data and the experimental data in the low frequency range were smaller than those in the high frequency range. Therefore, sound absorbing coefficients of the investigated multilayer microperforated panels in the high frequency range of 1000-6000 Hz were compared, as shown in Fig. 10. The standard deviations of theoretical data and the experimental data were 13.84, 5.42, 7.54, and 8.43 for the multilayer microperforated panels with layer number of 1, 2, 3, and 4, respectively. The major reason for this phenomenon was that the sound absorption process in the high frequency range was more sensitive to the fabrication error, the theoretical error, and the measurement error than that in the low frequency range.

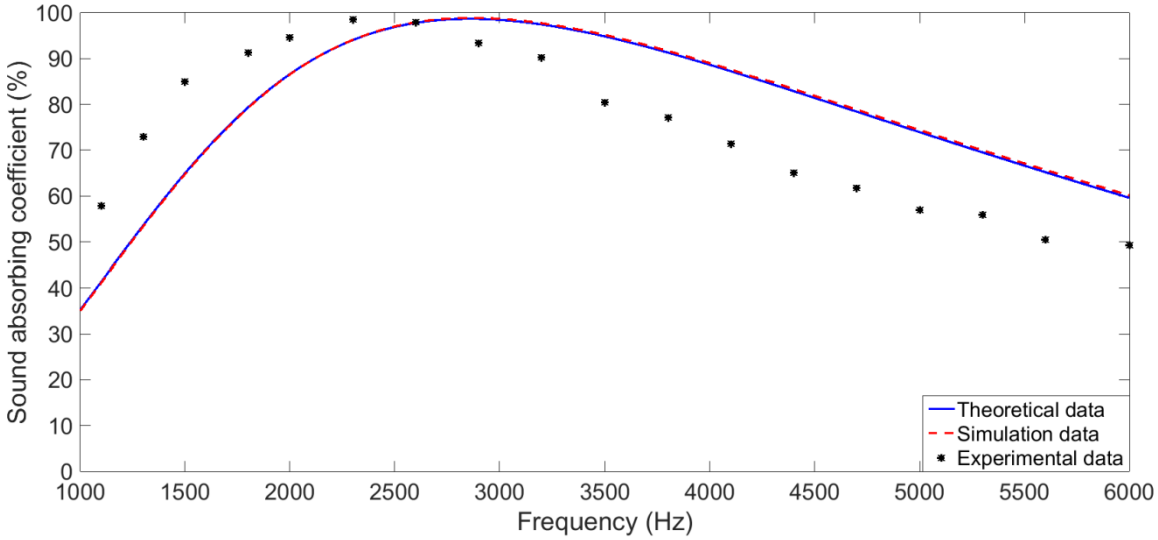

(a) Microperforated panel with 1 layer

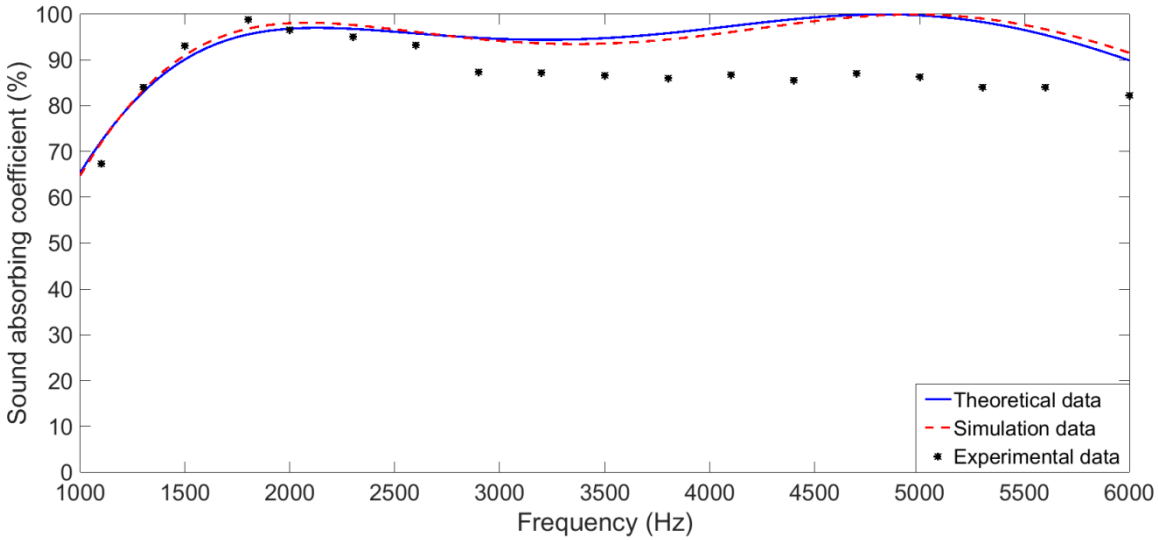

(b) Multilayer microperforated panel with 2 layers

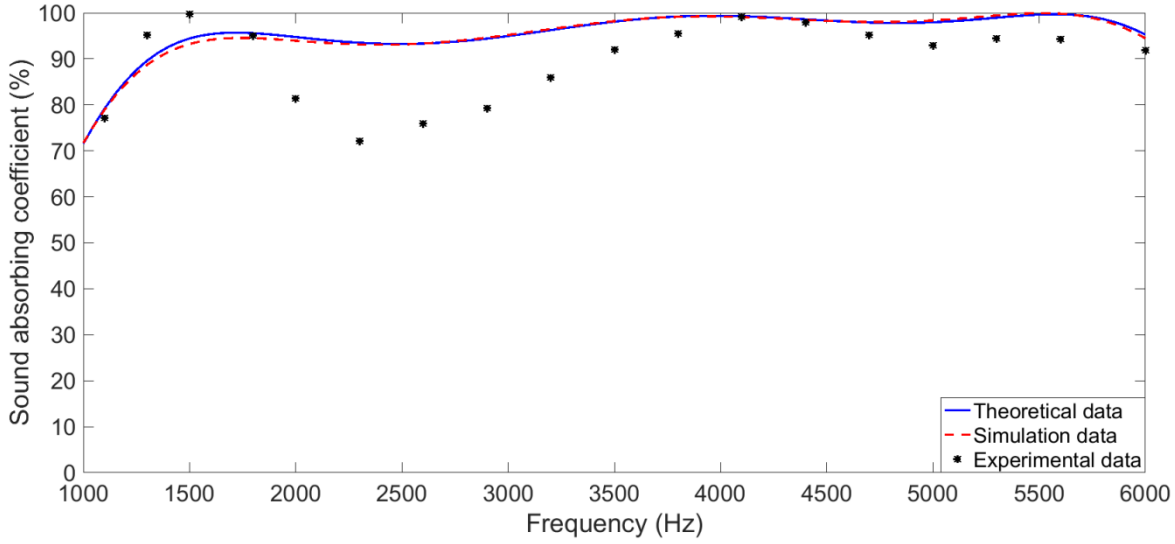

(c) Multilayer microperforated panel with 3 layers

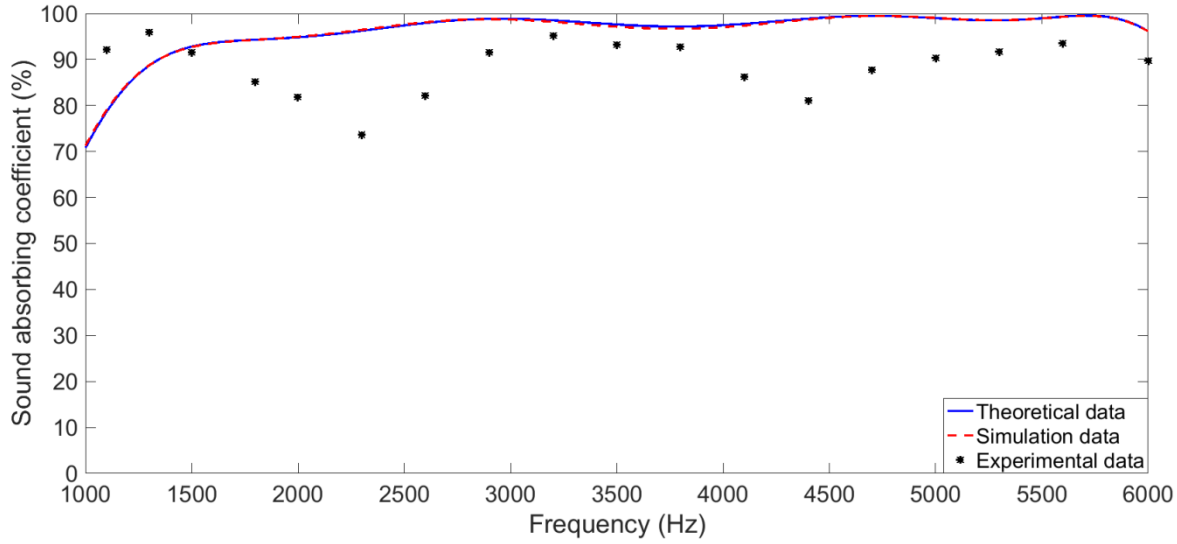

(d) Multilayer microperforated panel with 4 layers

Fig. 10. Comparisons of sound absorbing coefficients of the investigated multilayer microperforated panels in the high frequency range of 1000-6000 Hz

Through exchanging the first and second panels in the multilayer microperforated panels with layer number of 2, 3, and 4, respectively, sound absorbing coefficient of the contrasted sample was tested to further validate effectiveness of the optimization process, as shown in Fig. 11. The average sound absorbing coefficients for the contrasted multilayer microperforated panels with layer number of 2, 3, and 4 were 57.92%, 52.63%, and 60.02%, respectively, which were significantly smaller than that of

the optimal multilayer microperforated panels with layer number of 2, 3, and 4. This result further proved that optimization of the structural parameters was effective and essential.

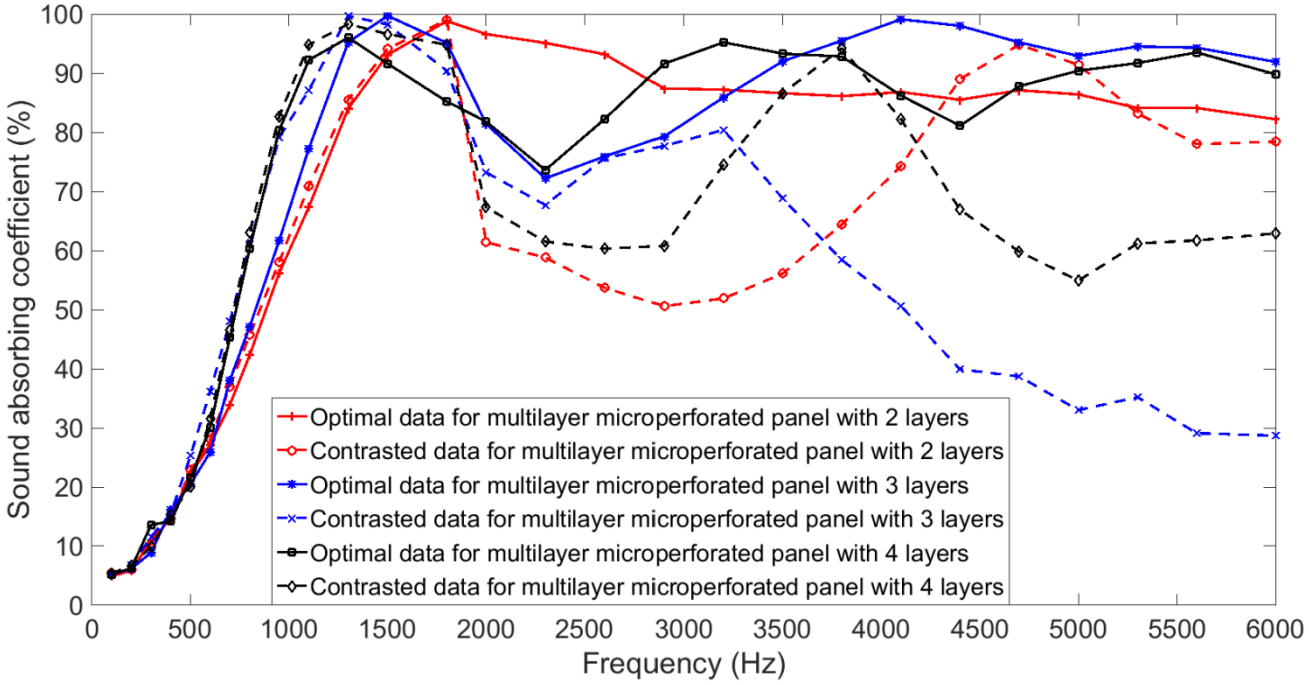

Fig. 11. Comparison of the optimal data and the contrasted data for multilayer microperforated panel

6. Conclusions

Optimal design and experimental validation of the sound absorbing multilayer microperforated panel with constraint conditions was conducted in this study. Through the theoretical modeling, parameter optimization, analog simulation, and experimental validation, an effective method for development of the desired sound absorber was proposed, and the following conclusions were obtained.

(1) A theoretical model was constructed based on the Maa's theory to quantificational describe the relationship between the sound absorbing coefficient of the multilayer microperforated panel and its structural parameters, which provide the theoretical basis for the further optimal design.

(2) Structural parameters of the multilayer microperforated panel were optimized through the cuckoo search algorithm with the constraint conditions, and the theoretical optimal average sound absorbing coefficients in frequency range of 100-6000 Hz were 69.79%, 84.30%, 85.52%, 85.74%, 85.77%,

85.87%, 85.91%, and 85.98% corresponding to multilayer microperforated panel with layer number of 1 to 8, which provide guidance for the fabrication process.

(3) The achieved optimal parameters were introduced into the analog simulation model according to the finite element method, and the simulation results were well consistent with the theoretical results in each frequency point, and the differences were kept in ±2.5%, which preliminary verified the accuracy and effectiveness of the parameter optimization.

(4) The obtained optimal design of multilayer microperforated panel with no more than 4 layers was finally validated by testing experiments based on the standing wave method, and the optimal average sound absorbing coefficients in the frequency range of 100-6000 Hz were 57.21%, 66.29%, 68.33%, and 69.36%, respectively. Evolution trends of the actual sound absorbing coefficients were generally consistent with that of the theoretical data and that of the simulation data, though there existed some deviations generated by the fabrication error, the theoretical error, and the measurement error.

It can be concluded that the sound absorption performance of the multilayer microperforated panel is significantly improved through the parameter optimization, which will be propitious to promote the applications of the multilayer microperforated panel products in the field of noise reduction.

Acknowledgements

This work was supported by a grant from National Natural Science Foundation of China (Grant No. 51505498), a grant from Natural Science Foundation of Jiangsu Province (Grant No. BK20150714), and a grant from National Key R & D Program of China (Grant No. 2016YFC0802900). Xinmin Shen was grateful for support from the Hong Kong Scholars Program (No. XJ2017025).

References

[1] D.Y. Maa, Potential of microperforated panel absorber, J. Acoust. Soc. Am. 104(5) (1998)

2861-2866.

[2] Y.K. Chiang, Y.S. Choy, Acoustic behaviors of the microperforated panel absorber array in nonlinear regime under moderate acoustic pressure excitation, J. Acoust. Soc. Am. 143(1) (2018) 538-549.

[3] H.S. Kim, P.S. Ma, S.R. Kim, S.H. Lee, Y.H. Seo, A model for the sound absorption coefficient of multi-layered elastic microperforated plates, J. Sound. Vib. 430 (2018) 75-92.

[4] P.V. Bansod, T.S. Teja, A.R. Mohanty, Improvement of the sound absorption performance of jute felt-based sound absorbers using microperforated panels, J. Low. Freq. Noise. V. A. 36(4) (2017) 376-389.

[5] X.L. Gai, X.H. Li, B. Zhang, T. Xing, J.J. Zhao, Z.H. Ma, Experimental study on sound absorption performance of microperforated panel with membrane cell, Appl. Acoust. 110 (2016) 241-247.

[6] M. Toyoda, S. Fujita, K. Sakagami, Numerical analyses of the sound absorption of cylindrical microperforated panel space absorbers with cores, J. Acoust. Soc. Am. 138(6) (2015) 3531-3538.

[7] D.Q. Chang, F. Lu, W.N. Jin, B.L. Liu, Low-frequency sound absorptive properties of double-layer perforated plate under grazing flow, Appl. Acoust. 130 (2018) 115-123.

[8] M. Yang, P. Sheng, Sound Absorption Structures: From Porous Media to Acoustic Metamaterials, Annu. Rev. Mater. Res. 47 (2017) 83-114.

[9] S.T. Liu, W.J. Chen, Y.C. Zhang, Design optimization of porous fibrous material for maximizing absorption of sounds under set frequency bands, Appl. Acoust. 76 (2014) 319-328.

[10] T. Okuzono, K. Sakagami, Room acoustics simulation with single-leaf microperforated panel absorber using two-dimensional finite-element method, Acoust. Sci. & Tech. 36(4) (2015) 358-361.

[11] J. Liu, X. Hua, D.W. Herrin, Estimation of effective parameters for microperforated panel absorbers and applications, Appl. Acoust. 75 (2014) 86-93.

[12] T. Okuzono, K. Sakagami, A frequency domain finite element solver for acoustic simulations of 3D rooms with microperforated panel absorbers, Appl. Acoust. 129 (2018) 1-12.

[13] Y.F. Tang, F.H. Li, F.X. Xin, T.J. Lu, Heterogeneously perforated honeycomb-corrugation hybrid sandwich panel as sound absorber, Mater. Des. 134 (2017) 502-512.

[14] Y.F Tang, S.W. Ren, H. Meng, F.X. Xin, L.X. Huang, T.N. Chen, C.Z. Zhang, T.J. Lu, Hybrid acoustic metamaterial as super absorber for broadband low-frequency sound, Sci. Rep. 7 (2017) 43340.

[15] D.Y. Maa, Theory and design of microperforated panel sound-absorbing constructions, Scientia Sinica 18(1) (1975) 55-71.

[16] D.Y. Maa, Design of microperforated panel constructions, Acta Acustica 13(3) (1988) 174-180.

[17] J.F. Ning, S.W. Ren, G.P. Zhao, Acoustic properties of microperforated panel absorber having arbitrary cross-sectional perforations, Appl. Acoust. 111 (2016) 135-142.

[18] Y.J. Qian, J. Zhang, N. Sun, A strategy for extending the effective application of microperforated panel absorbers to high sound intensity, Appl. Acoust. 130 (2018) 124-127.

[19] X.D. Zhao, X. Wang, Y.J. Yu, Enhancing low-frequency sound absorption of microperforated panel absorbers by combining parallel mechanical impedance, Appl. Acoust. 130 (2018) 300-304.

[20] Z.Q. Liu, J.X. Zhan, M. Fard, J.L. Davy, Acoustic properties of a porous polycarbonate material produced by additive manufacturing, Mater. Lett. 181 (2016) 296-299.

[21] T. Bravo, C. Maury, C. Pinhède, Enhancing sound absorption and transmission through flexible multi-layer microperforated structures, J. Acoust. Soc. Am. 134(5) (2013) 3663-3673.

[22] H. Ruiz, P. Cobo, F. Jacobsen, Optimization of multiple-layer microperforated panels by simulated annealing, Appl. Acoust. 72(10) (2011) 772-776.

[23] X.D. Zhao, P. Hu, P. Sun, The comparative analyses of the calculation methods for absorptivity of multilayer microperforated panel absorbers, J. Appl. Acoust. 31(3) (2012) 196-201.

[24] X.D. Zhao, X.J. Zhang, Z. Jiang, Three layer microperforated panel optimal design and analysis of its characteristic, Acta Acustica 33(1) (2008) 84-87.

[25] C.Q. Wang, L.X. Huang, Y.M. Zhang, Oblique incidence sound absorption of parallel arrangement of multiple microperforated panel absorbers in a periodic pattern, J. Sound. Vib. 333(25) (2014) 6828-6842.

[26] H. Meng, F.X. Xin, T.J. Lu, Sound absorption optimization of graded semi-open cellular metals by adopting the genetic algorithm method, J. Vib. Acoust. 136 (2014) 061007.

[27] Q.B. Ao, J.Z. Wang, H.P. Tang, H. Zhi, J. Ma, T.F. Bao, Sound absorption characteristics and structure optimization of porous metal fibrous materials, Rare Metal Mat. Eng. 44(11) (2015) 2646-2650.

[28] W.H. Chen, T.N. Chen, F.X. Xin, X.P. Wang, X.W. Du, T.J. Lu, Modeling of sound absorption based on the fractal microstructures of porous fibrous metals, Mater. Des. 105 (2016) 386-397.

[29] S.T. Liu, W.J. Chen, Y.C. Zhang, Design optimization of porous fibrous material for maximizing absorption of sounds under set frequency bands, Appl. Acoust. 76 (2014) 319-328.

[30] J.L. Zhu, J. Sun, H.P. Tang, J.Z. Wang, Q.B. Ao, T.F. Bao, W.D. Song, Gradient-structural optimization of metal fiber porous materials for sound absorption, Powder Technol. 301 (2016) 1235-1241.

[31] X.S. Yang, S. Deb, Multiobjective cuckoo search for design optimization, Comput. Oper. Res.

40(6) (2013) 1616-1624.

[32] X.S. Yang, S. Deb, Cuckoo search: recent advances and applications, Neural. Comput. & Applic. 24(1) (2014) 169-174.

[33] M.-A. Gaudreau, F. Sgard, F. Laville, H. Nélisse, A finite element model to improve noise reduction based attenuation measurement of earmuffs in a directional sound field, Appl. Acoust. 119 (2017) 66-77.

[34] K. Carillo, F. Sgard, O. Doutres, Numerical study of the broadband vibro-acoustic response of an earmuff, Appl. Acoust. 134 (2018) 25-33.

[35] X.C. Yang, K. Peng, X.M. Shen, X.N. Zhang, P.F. Bai, P.J. Xu, Geometrical and dimensional optimization of sound absorbing porous copper with cavity, Mater. Des. 131 (2017) 297-306.

[36] P.F. Bai, X.M. Shen, X.N. Zhang, X.C. Yang, Q. Yin, A.X. Liu, Influences of Compression Ratios on Sound Absorption Performance of Porous Nickel-Iron Alloy, Metals 8(7) (2018) 539.

[37] D.H. Lee, Y.P. Kwon, Estimation of the absorption performance of multiple layer perforated panel systems by transfer matrix method, J. Sound. Vib. 278(4-5) (2004) 847-860.

[38] K. Verdière, R. Panneton, S. Elkoun, Transfer matrix method applied to the parallel assembly of sound absorbing materials, J. Acoust. Soc. Am. 134(6) (2013) 4648-4658.

[39] T. Du, T.C. Miao, G.T. Fu, D.Z. Wu, Study on Numerical Simulation Method for the MPP Absorber, Journal of Engineering Thermophysics 36(6) (2015) 1242-1246.

[40] A.H. Gandomi, X.S. Yang, A.H. Alavi, Cuckoo search algorithm: a metaheuristic approach to solve structural optimization problems, Eng. Comput.-Germany 29(1) (2013) 17-35.

[41] A.R. Yildiz, Cuckoo search algorithm for the selection of optimal machining parameters in milling operations, Int. J. Adv. Manuf. Technol. 64(1-4) (2013) 55-61.

[42] A. Ouaarab, B. Ahiod, X.S. Yang, Discrete cuckoo search algorithm for the travelling salesman problem, Neural. Comput. & Applic. 24(7-8) (2014) 1659-1669.